

Role of Planetary Waves in the Stratosphere-troposphere Coupled Variability in the Northern Hemisphere Winter

Yuhji Kuroda and Kunihiro Kodera

Climate Research Department, Meteorological Research Institute, Tsukuba, Japan

Abstract. The role of planetary waves in stratosphere-troposphere coupled variability is investigated using an extended singular value decomposition analysis of zonal-mean zonal wind and the vertical component of the Eliassen-Palm (E-P) flux for the winters from 1979/80 to 1995/96. The results suggest a close relationship between anomalies of zonal-mean zonal wind and the convergence zone of E-P flux, which together shift poleward and downward from the stratosphere to the troposphere as time advances. Following enhanced vertical propagation of waves into the stratosphere, the Arctic Oscillation (AO) pattern is seen in the 500 hPa geopotential height field in association with an increased poleward propagation of tropospheric waves.

1. Introduction

During northern hemisphere winter, the stratospheric and tropospheric circulations are closely coupled from interseasonal to interannual time scales [e.g., *Perlwitz et al.*, 1995; *Kodera*, 1995; *Baldwin and Dunkerton*, 1994]: i.e., the strength of the polar-night jet (or polar vortex) is highly correlated with the so-called Arctic Oscillation, as characterized by a seesaw in tropospheric geopotential height between the Arctic and mid-latitudes [*Thompson and Wallace*, 1998]. On interseasonal (i.e., month to month) time scales, the downward propagation of zonal wind anomalies from the stratosphere appear to produce the AO signal seen in the troposphere [*Kodera and Koide*, 1997; *Kodera et al.*, 1999; *Baldwin and Dunkerton*, 1999].

Generally speaking, the winter stratosphere is coupled with the troposphere through the interaction of waves originating from the troposphere driving a meridional circulation in the stratosphere [e.g., *Haynes et al.*, 1991]. In the case of stratospheric sudden warmings [*Matsuno*, 1971], the role of troposphericly originating planetary waves is clear, however, in the case of the more slowly evolving AO, the role of planetary waves in coupling the troposphere and stratosphere is much less clear [*Thompson and Wallace*, 1998]. The purpose of the present study is to clarify the role of planetary waves in stratosphere-troposphere coupled variability, particularly in the context of the AO.

2. Data and method of analysis

The stratosphere and troposphere data used in the present study are updated from *Kuroda and Kodera* [1998]. Original data are analyzed by U.S. National Center for Environmental

Prediction (NCEP)/Climate Prediction Center (CPC) (formerly NMC/CAC). Tropospheric data below 100 hPa are due to the analysis of NCEP, while stratospheric data are calculated from satellite-derived geopotential height produced by CPC as documented in *Randel* [1992]. All calculations are on monthly mean data except for those involving E-P and wave activity fluxes (see *Andrews et al.*, 1987 and *Plumb*, 1985, respectively), which were performed on a 5 day-mean and then monthly averaged. The 17 winters from 1979/80 to 1995/96 are considered.

To extract dominant mode of common variability from two fields, singular value decomposition (SVD) analysis is widely used [*Bretherton et al.*, 1992]. As we treat a propagating phenomenon in the present study, not only the simultaneous correlation but also the lagged correlation should be taken into account. For this purpose, a SVD analysis based on an extended vector, which incorporates lagged vectors into the original one, is treated. This technique, extended SVD (E-SVD), is the direct extension of the extended empirical orthogonal function (E-EOF) [*Weare and Nasstrom*, 1982] analysis used for a single field.

In the present study, an E-SVD analysis of zonal-mean zonal wind and the vertical component of the E-P flux is performed. The extended vector is constructed by adding up to two months of lag as follows;

$$\mathbf{x}(t) = (\mathbf{a}(t), \mathbf{a}(t+1), \mathbf{a}(t+2)).$$

Here t is time in months, and $\mathbf{a}(t)$ is monthly mean zonal-mean zonal wind or the vertical component of the E-P flux at each height and latitude. Because we focus mainly on wintertime, covariances are calculated using data belonging to a cold season (November to February). It should be noted that all variables are normalized by their variance prior to the SVD analysis to cover the large range of pressure levels. A SVD of a large cross-covariance matrix of tripled space dimension due to the inclusion of delayed components can be efficiently performed by the method of *Kuroda* [1998].

3. Results

The squared covariance fraction of the leading SVD mode as defined above is 42% and is well separated from the second mode (explaining 20%). The correlation coefficient between the respective expansion coefficients is 0.90. The leading SVD is shown in Figure 1 as heterogeneous regression maps. Note that the meridional component of the E-P flux was constructed by regression against the zonal-mean zonal wind expansion coefficient. The E-P flux vectors are scaled by the inverse square root of pressure. The panels in Figure 1 are for 0, 1, and 2 month lags (reading from left to right). Regions where the correlation coefficients exceed the 95% significance level (0.34) are shaded.

Copyright 1999 by the American Geophysical Union.

Paper number 1999GL900507.
0094-8276/99/1999GL900507\$05.00

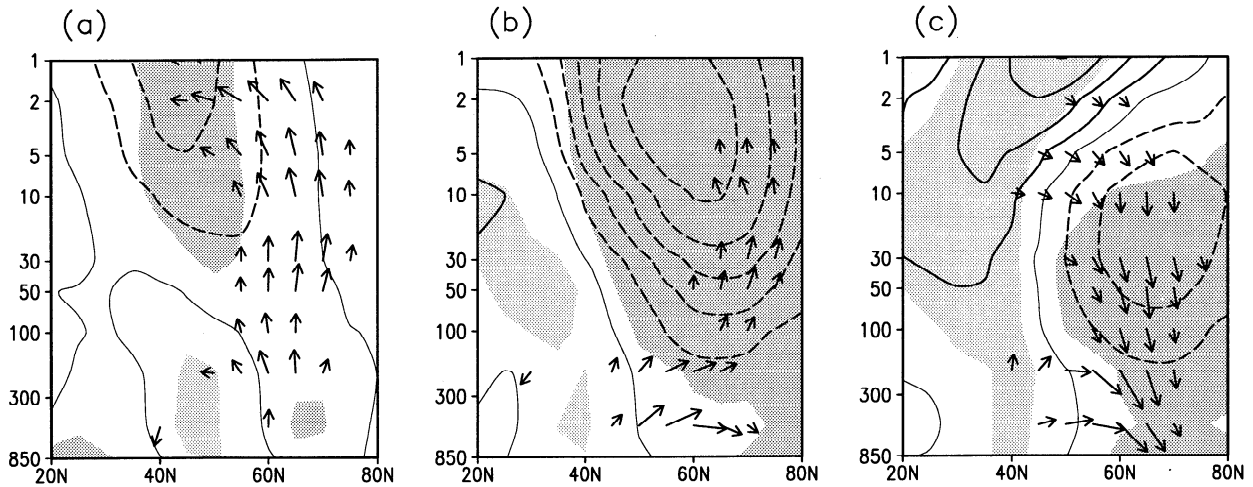


Figure 1. Heterogeneous regression map of the leading E-SVD between the zonal-mean zonal wind (contoured) and the vertical component of E-P flux (vectors). Meridional component of the E-P flux is constructed by regression against the expansion coefficient of the zonal-mean zonal wind. Panels a, b, and c correspond to lags 0, 1 and 2 months, respectively. Shading denotes regions where the heterogeneous correlation of zonal winds are significant at the 95% level. The contour interval is 2 ms^{-1} and the dashed lines indicate negative values. Zero contour line is shown by the thin line. The E-P flux is scaled by the inverse square root of pressure and small arrows are not plotted.

At lag 0 (Figure 1a), weak negative anomalies in the zonal-mean zonal wind are seen in the mid-latitude upper stratosphere near 45°N . Enhanced E-P flux directed from the high-latitude troposphere towards a center of negative zonal-mean zonal wind anomaly in the upper stratospheric is noted. At lag 1 (Figure 1b), the negative anomalies of zonal-mean zonal winds amplify while shifting poleward and downward. Together with the poleward and downward shift of negative wind anomalies, E-P flux vectors are directed more poleward. Note also that in the troposphere, poleward propagation of wave activity increases. At lag 2 (Figure 1c), the negative zonal wind anomalies in high-latitudes move further downward into the troposphere, while at the same time low-latitude positive anomalies now extend up and poleward, covering almost all the upper stratosphere. Downward directed anomalous E-P flux in the polar region indicates a weakening of wave activity in the stratosphere. It should be noted that enhanced poleward propagation of the E-P flux in the troposphere seen at lag 1 persists at lag 2.

In order to investigate in more detail how the tropospheric circulation evolves, the 500-hPa geopotential height and wave activity flux [Plumb, 1985] are regressed against the expansion coefficient of the zonal-mean zonal wind of the leading SVD (Figure 2). Note that the zonally averaged Plumb flux is precisely the E-P flux shown in Figure 1. Since our focus here is on planetary waves, the wave activity flux is calculated after truncation at zonal wave-number five.

At lag 0 (Figure 2a), positive and negative centers of height anomaly are found over the northern part of Eurasia. Longitude-height cross-section of wave activity flux at 60°N (averaged between 50°N - 70°N) (Figure 3a) shows that the enhanced vertical propagation of waves seen in Figure 1a occurs over a rather confined region of the Eurasian sector, suggesting that 500 hPa height anomalies over the Eurasian sector are a source of enhanced planetary wave activity. On the other hand, the mid-latitude height anomalies seen over the Atlantic sector are apparently not related to the enhanced vertical propagation observed.

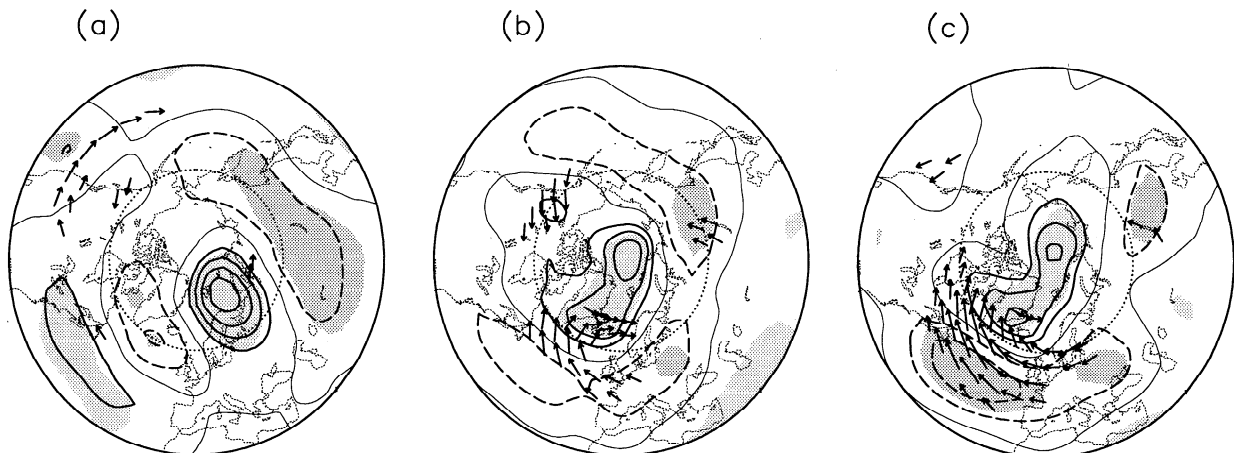


Figure 2. The same as in Figure 1 except for 500-hPa geopotential height (contoured) and the wave activity flux (vectors). Contour interval is 15 m. Latitudinal circles indicate 60°N and 30°N .

At lag 1 (Figure 2b), geopotential height anomalies become more zonally symmetric. The increase of geopotential height over the Arctic and lowering over the mid-latitudes is consistent with a formation of the meridional dipole pattern of anomalous zonal wind shown in Figure 1b. It should be noted that this pattern is very similar to the AO signal at 500 hPa [as seen in Figure 1 of *Thompson and Wallace, 1998*]. The lowering of geopotential height over the Atlantic and eastern Siberian sectors, and increased height over Alaska both correspond to the poleward propagation of waves seen in Figure 1b, (although only the Siberian height anomalies are seen to be significant).

At lag 2 (Figure 2c), the North Atlantic Oscillation (NAO) pattern becomes more prominent while the south-eastward propagation of wave activity decreases in the Atlantic sector. Regression of time filtering data shows that this decrease corresponds to the reduced amplitude of high frequency waves (not shown).

4. Discussion and concluding remarks

An E-SVD analysis between the zonal-mean zonal wind and vertical component of E-P flux was conducted for the period from 1979/80 to 1995/96. To examine the stability of the leading SVD mode, similar analyses are repeated by dividing the data into two parts. However, characteristics of the evolution of the zonal-mean zonal wind and the E-P flux described above are conserved. We therefore consider that the

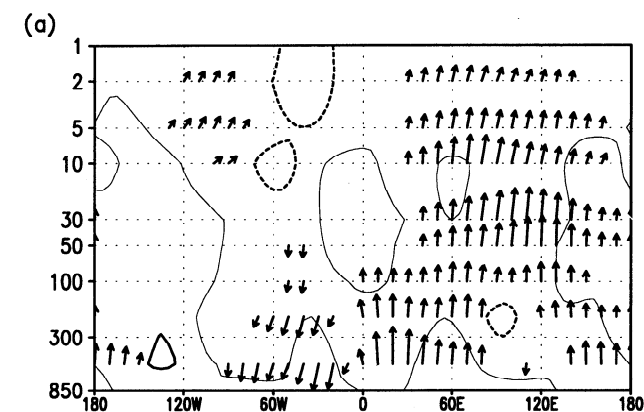


Figure 3. The same as in Figure 1a, but for Plumb's wave activity flux averaged around 60°N. The vertical and zonal components of wave activity flux are shown as arrows, while the meridional component is contoured. Contour intervals are 15 and the arrow at the right-bottom corresponds to 30 with relative unit. Zero contour line is shown by the thin line.

present analysis represents the natural mode of variability in the atmosphere.

The leading SVD shows poleward and downward propagation of zonal-mean zonal wind anomalies together with anomalous E-P flux vectors toward negative anomalies of zonal-mean zonal wind (Figure 1). To investigate a closer

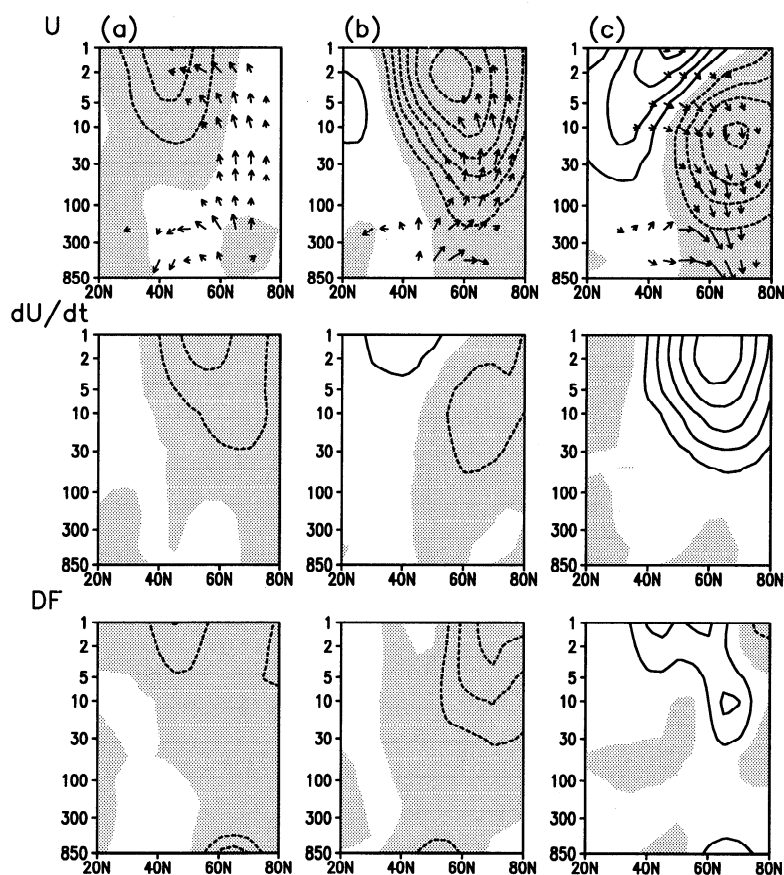


Figure 4. (Top panels) The same as in Figure 1, but for the regression map of the leading E-SVD based on the pentad mean data. Panels a, b, and c display components of lags 3, 9, 15 pentads, respectively (see text). Middle and bottom panels are the same as in top panels, but for the zonal-mean zonal wind tendency and the E-P flux divergence, respectively. Contour intervals are 2 ms⁻¹ (top panels), 0.2 ms⁻¹day⁻¹ (middle panels), and 1 ms⁻¹day⁻¹ (bottom panels). Zero counter line is omitted and negative values are shaded.

relationship between the zonal-mean zonal wind and wave activity, an E-SVD analysis is conducted using finer resolution of pentad (5-day) mean data. Similar to the monthly mean case, a lagged correlation matrix is calculated using data belonging to the cold season (November to February). The leading SVD of present analysis includes 18 components of lags 0 to 17 pentad. Regression patterns of monthly mean data in Figs. 1a, 1b, and 1c, should correspond to those of lags 3, 9, 15 pentads shown in the top panels in Fig. 4a, 4b, and 4c, respectively. It can easily be seen that almost an identical regression pattern is reproduced with 5-day mean data. In Figure 4, zonal-mean zonal wind tendency (du/dt) and acceleration due to E-P flux divergence (DF) calculated from regressed fields are also shown in the middle and bottom panels, respectively. Similarity of the patterns between du/dt and DF strongly suggests that this mode of variability is produced through wave-mean flow interaction.

An AO pattern is apparent during the second and third stage of our analysis. However, if one investigates wave activity only during this period, the role of vertical propagation of the anomalous E-P flux becomes unclear because the anomalous E-P fluxes direct upward (Figure 1b) for one period, but downward (Figure 1c) for the other period. In fact, vertical propagation of waves takes place earlier than the formation of the AO pattern. A pair of geopotential height anomalies over the Eurasian sector is associated with the vertical propagation of waves and it is different from the AO pattern (Figure 1a). It is interesting to examine why the enhanced vertical wave propagation takes place over the Siberian sector for the first stage.

The AO pattern, as characterized by a seesaw in 500 hPa geopotential height between the Arctic and mid-latitudes, appears (Figure 2b and 2c) when a meridional dipole anomaly in zonal-mean zonal wind forms in the troposphere together with poleward directed anomalous E-P flux (Figures 1b and 1c). The regional geopotential height anomalies in the mid-latitudes appear related to changes in the meridional propagation of tropospheric waves [Kodera *et al.*, 1996]. It should be noted that the convergence of E-P flux in the Arctic tends to maintain the meridional seesaw pattern of the AO.

The poleward propagation of the anomalous E-P flux is also seen at lag 1 and lag 2, although the strength of the lower stratospheric polar night jet and the vertical propagation of waves have been changed, suggesting that the anomalous zonal wind structure is sustained by tropospheric processes. The geopotential height pattern seen over the Atlantic region (Figure 2c) exhibits a more NAO-like structure at lag 2, and the decreased eastward propagation of quasi-stationary wave activity suggests a possible role of the transient eddy activity in maintaining tropospheric zonal wind anomalies. This should be verified in a future study.

To conclude, it is noted that the stratosphere-troposphere coupled mode of variability seen here has large amplitude during the winter when major stratospheric warming takes place. The relationship between stratospheric sudden

warmings and the slowly evolving zonal-wind anomalies studied here will be treated in a separate paper.

Acknowledgments. The authors wish to thank Dr. J. Fyfe and anonymous referees for their critical comments on the original manuscript. This study was supported in part by the Japan Science and Technology Agency research program on stratospheric change and its role in climate.

References

- Andrews, D.G., J.R. Holton, and C.B. Leovy, *Middle atmosphere dynamics*, Academic Press, 489pp., 1987.
- Baldwin, M.P., X. Cheng and T.J. Dunkerton, Observed correlation between winter-mean tropospheric and stratospheric circulation anomalies, *Geophys. Res. Lett.*, **21**, 1141-1144, 1994.
- Baldwin, M. P., and T. J. Dunkerton, Propagation of the Arctic Oscillation from the stratosphere to the troposphere, *J. Geophys. Res.*, submitted, 1999.
- Bretherton, C.S., C. Smith, and J.M. Wallace, An intercomparison of methods for finding coupled patterns in climate data, *J. Clim.*, **5**, 541-560, 1992.
- Haynes, P.H., C.J. Marks, M.E. McIntyre, T.G. Shepherd, and K.P. Shine, On the "Downward control" of extratropical diabatic circulations by eddy-induced mean zonal forces, *J. Atmos. Sci.*, **48**, 651-678, 1991.
- Kodera, K., H. Koide, and H. Yoshimura, Northern hemisphere winter circulation associated with the North Atlantic Oscillation and stratospheric polar night jet, *Geophys. Res. Lett.*, **26**, 443-446, 1999.
- Kodera, K., and H. Koide, Spatial and seasonal characteristics of recent decadal trends in the northern hemispheric troposphere and stratosphere, *J. Geophys. Res.*, **102**, 19433-19447, 1997.
- Kodera, K., M. Chiba, H. Koide, A. Kitoh, and Y. Nikaidou, Interannual variability of the winter stratosphere and troposphere in the Northern Hemisphere, *J. Meteorol. Soc. Jpn.*, **74**, 365-382, 1996.
- Kodera K., On the origin and nature of the interannual variability of the winter stratosphere circulation in the northern hemisphere. *J. Geophys. Res.*, **100**, 14,077-14,087, 1995.
- Kuroda Y. and K. Kodera, Interannual variability in the troposphere and stratosphere of the southern hemisphere winter. *J. Geophys. Res.*, **103**, 13,787-13,799, 1998.
- Kuroda Y., An effective SVD calculation method for climate analysis. *J. Meteorol. Soc. Jpn.*, **76**, 649-655, 1998.
- Matsuno T., A dynamical model of the stratospheric sudden warming. *J. Atmos. Sci.*, **28**, 1479-1494, 1971.
- Perlwitz, J., and H-F. Graf, The statistical connection between tropospheric and stratospheric circulation of the Northern Hemisphere in winter. *J. Clim.*, **8**, 2281-2295, 1995.
- Plumb, R.A., On the three-dimensional propagation of stationary waves. *J. Atmos. Sci.*, **42**, 217-229, 1985.
- Randel, W.J., *Global atmospheric circulation statistics, 1000-1 mb*. NCAR/TN-366+STR, NCAR Technical Note, 256pp, 1992.
- Tompson D.W.J. and J.M. Wallace, The Arctic oscillation signature in the wintertime geopotential height and temperature fields. *Geophys. Res. Lett.*, **25**, 1297-1300, 1998.
- Weare, B. C., and J. S. Nasstrom, Examples of extended empirical orthogonal function analysis, *Mon. Weather Rev.*, **110**, 481-485, 1982.

Y. Kuroda, and K. Kodera, Meteorological Research Institute, 1-1 Nagamine, Tsukuba, 305-0052 Japan. (E-mail: kuroda@mri-jma.go.jp; kodera@mri-jma.go.jp)

(Received: April 14, 1999; revised June 9, 1999; accepted June 14, 1999.)